Development of a Microplasma-Based Heaterless, Insertless, Cathode

IEPC-2017-183

Presented at the 35th International Electric Propulsion Conference
Georgia Institute of Technology • Atlanta, Georgia • USA
October 8 – 12, 2017

Ryan P. Gott[1] and Kunning G. Xu[2]
Department of Mechanical and Aerospace Engineering, University of Alabama in Huntsville, Huntsville, Alabama, 35816, United States

A heaterless, insertless hollow cathode has been developed by using an argon microplasma generated in a quartz tube with a tungsten filament and brass ion collector. The cathode produced milliamps of current at an anode voltage of 300 V. Various power sources and inputs, tube sizes, and flow rates have been analyzed and tested. Operating conditions such as current output, electron temperature, and electron density of the cathode have been characterized in testing at the University of Alabama in Huntsville.

Nomenclature

A_p = Langmuir probe surface area
A_t = Tube exit area
Γ = current flux
k = Boltzmann's constant
i_n = saturation current
M = mass of Argon
$n_{e,i,0}$ = electron, ion, and neutral density
q = electron charge
T_e = electron temperature

I. Introduction

HALL Effect Thrusters (HET) and Ion Thrusters use the expulsion of positively charged ions to generate thrust. In order to prevent this beam from negatively charging the thrusters, a beam of electrons is used to neutralize the ions[1]. Several types of cathodes have been developed for these electric propulsion devices. Hollow cathodes are the most commonly used electron source due to their high electron density, long lifetime, and relatively low power requirements. However, the power required for most hollow cathodes is still too high for current and future small satellites. The component that draws the largest amount of power in a conventional hollow cathode is the heater. A heater is necessary to bring the thermoionic insert to its emission temperature. Heaterless cathodes have been studied previously[2–4], but require an insert material with a relatively low breakdown voltage. Insert materials, such as Barium Oxide and Lanthanum Hexaboride (LaB_6), have high rates of deterioration and thus limit the life of the cathode. The

[1] Graduate Research Assistant, Mechanical and Aerospace Engineering, rpg0007@uah.edu
[2] Assistant Professor, Mechanical and Aerospace Engineering, gabe.xu@uah.edu

contamination caused by the emissive materials also causes erosion and deterioration of the cathode. Additionally, external heaters require startup times that can exceed hundreds of seconds[5]. This is problematic because orbit control requires rapid ignition to be useful. A heaterless, insertless cathode is studied in this work that utilizes ac and pulsed dc electric fields to excite the propellant gas. This design helps to reduce power requirements which makes it easier to integrate into power limited small satellite electric propulsion.

II. Experimental Methods

A. Experimental Setup

Two experimental setups were used to measure operating conditions of the cathode. Electrical schematics for these two experiments can be seen in Figure 1 and Figure 2. A picture of the microplasma hollow cathode can be seen in Figure 3. Both experiments used ac and pulsed dc supplies. A commercial plasma ball was used as the ac supply and output a constant ac signal of 12 kV with a 1 µs pulse width and 11 kHz frequency. The pulsed dc supply was controlled by a high voltage pulse generator and digital delay generator and allowed for variation in voltage, pulse width, and frequency.

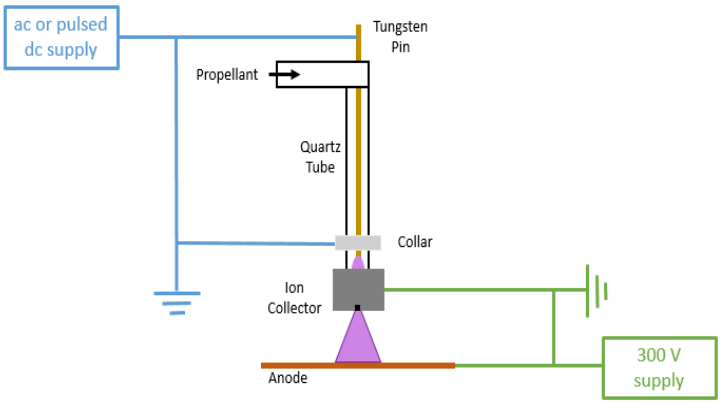

Figure 1. Electrical schematic of cathode. The design consists of two independent circuits.

The cathode was developed by inserting a 1 mm tungsten filament into a quartz tube. For initial tests, the quartz tube diameter was varied in the tests with either a 6 mm OD or ½" OD tube and different IDs. A steel collar was placed around the outside of the quartz tube and the microplasma was generated with an ac or pulsed dc power source connected to the central filament and external collar. A brass ion collector was placed on the end of the tube and connected to the negative terminal of a separate 300 V dc supply, while a plate anode was placed a short distance away and biased positively. Argon was used as the working gas and ionized by the induced field, then separated by the ion collector and anode. The flow of electrons into the anode produced a variety of currents.

Additional testing was done with Langmuir probes. For these tests, the probe replaced the anode, the 300V dc supply was not used, and the collar was removed. The probe was controlled with a sourcemeter. All tests were conducted in a vacuum chamber with a magnetically levitating turbopump. This was used to achieve high vacuum conditions that simulate the operating space environment. The chamber was pumped to 2 x 10^{-6} Torr base pressure for each test, with pressures reaching 4 x 10^{-4} Torr for higher flow rates.

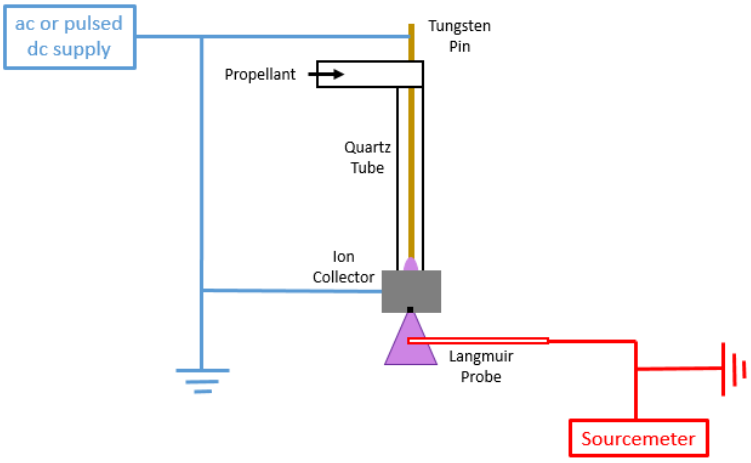

Figure 2. Electrical schematic of Langmuir probe tests.

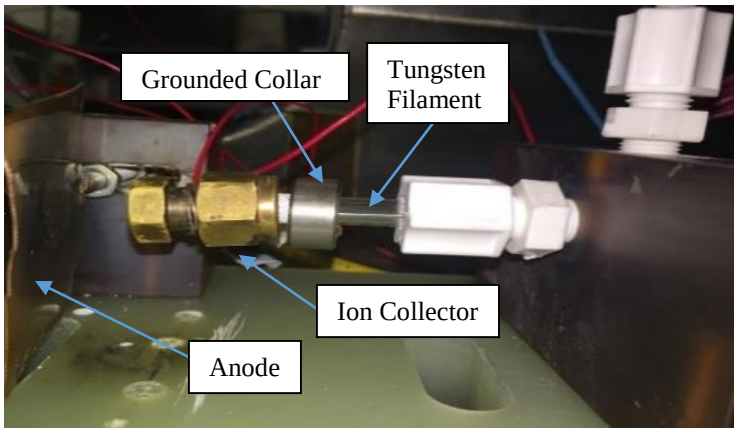

Figure 3. Hollow cathode setup.

B. Langmuir Probe Theory

Probe analysis assumes a collisionless plasma, meaning that the Debye length is less than the ion-neutral mean-free-path. This assumption holds true at low pressures, which allowed for the use of Langmuir probes in this experiment. In each test, a double probe was placed 5 mm from the cathode orifice and biased from -100 to 100 V using a Keithley 2400 sourcemeter. The filament current was measured and used to calculate electron temperature and density. Equation 1 shows that the change in current at 0 volts can be found using electron temperature, T_e, and the ion and electron saturation currents, i_1, and i_2, respectively[6].

$$\left.\frac{dI}{dV}\right]_0 = \frac{e}{kT_e}\frac{|i_1|*i_2}{|i_1|+i_2} \tag{1}$$

Where e is electron charge and k is Boltzmann's constant. This equation can be rearranged to solve for T_e, as shown in Equation 2.

$$\frac{1}{T_e} = \left.\frac{dI}{dV}\right]_0 \frac{k}{q}\frac{|i_1|+i_2}{|i_1|*i_2} \tag{2}$$

The change in current at zero volts and saturation currents can be found by using an I-V plot, as shown in Figure 4.

The change in current and saturation currents can be found by calculating three best fit lines on the plot. Two lines are fit to the positive and negative "legs" of the plot, while the third is through the zero voltage point. The saturation currents are the points of intersection of the three lines, while the change in current is the slope of the central line of best fit.

Under the assumption of quasi-neutrality, the ion density should be approximately equal to the electron density. Therefore, calculating the ion density will also give the electron density. Equation 3 shows the current relation to ion density, n_i.

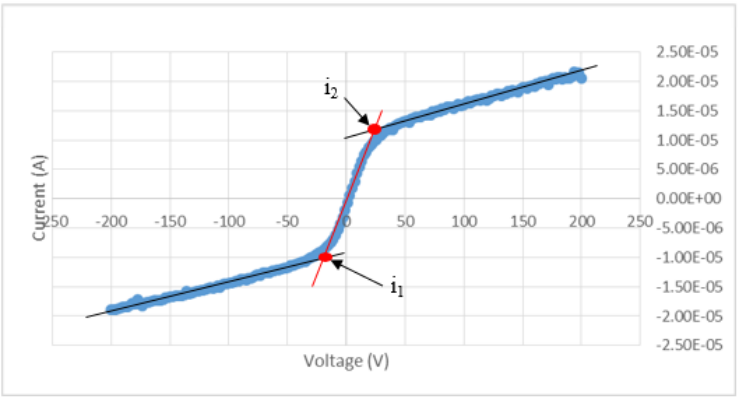

Figure 4. Sample graph for calculating T_e

$$I = \frac{1}{2} q n_i A_p \left(\frac{kT_e}{2\pi M}\right)^{\frac{1}{2}} \quad (3)$$

Where A is probe area and M is the mass of Argon. Rearranging to find n_i gives Equation 4.

$$n_i = \frac{2I}{qA_p\left(\frac{kT_e}{2\pi M}\right)^{\frac{1}{2}}} \quad (4)$$

The results of these calculations were used to characterize and compare operating conditions of the cathode.

III. Results

Tests were conducted to find the optimal mode of operation of the cathode. The first method of characterizing performance was measuring current output. The power supply used to provide voltage to the anode also provides a current readout. This readout was recorded for each experiment with different tube sizes and flow rates. Diagnostic techniques were also employed to compare modes of operation. Langmuir probes were used to measure electron temperature and density in a plasma.

C. Cathode Sizing

Sizing results are shown in Figure 5. The tests were run with the ac source and 300 V on the anode. It was found that the current increased with both flow rate and tube ID. While the desired flow rate is less than 30 sccm, there is no limit on tube ID. Further tests with 6 mm, 8 mm, and 10 mm ID tubes showed that performance stalled out at 6 mm, with minimal difference between 4 and 6 mm and a decrease at 8 and 10 mm. This is most likely related to a decrease in the density of the gas for larger IDs. The larger ID tubes have larger free volumes, allowing the plume to grow in the tube instead of at the anode. Additionally, the pressure within the tube is theoretically lower in the higher ID tubes. This prevents the plume from physically reaching the anode at the same conditions as the lower ID configurations.

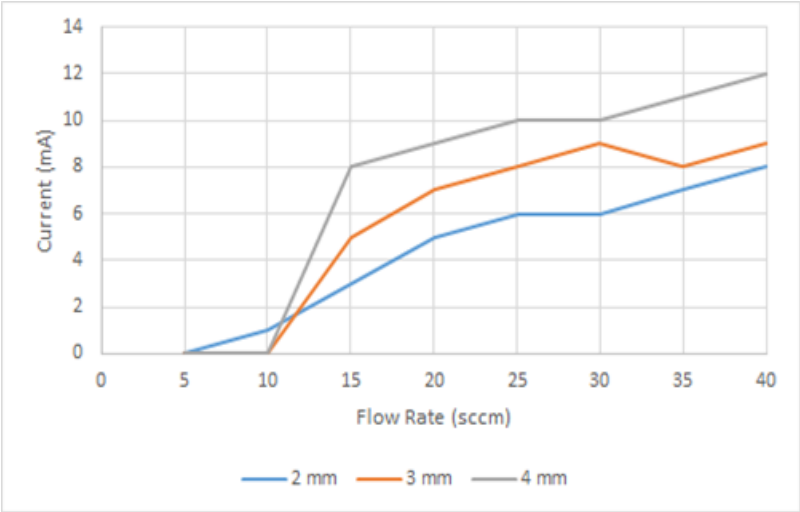

Figure 5. Comparison of operation with ac power. The lines denote different quartz tube inner diameters.

D. Langmuir Probe Measurements

Several Langmuir probe measurements were taken to calculate the properties of the ac source plasma. Three flow rates were tested, as shown in Figure 6. It can be seen that at positive voltages, the saturation current increases with flowrate. This is due to the higher density of particles available for ionization. Using Equations 2 and 4, the electron temperature and density for the ac source were found, as shown in Figure 7.

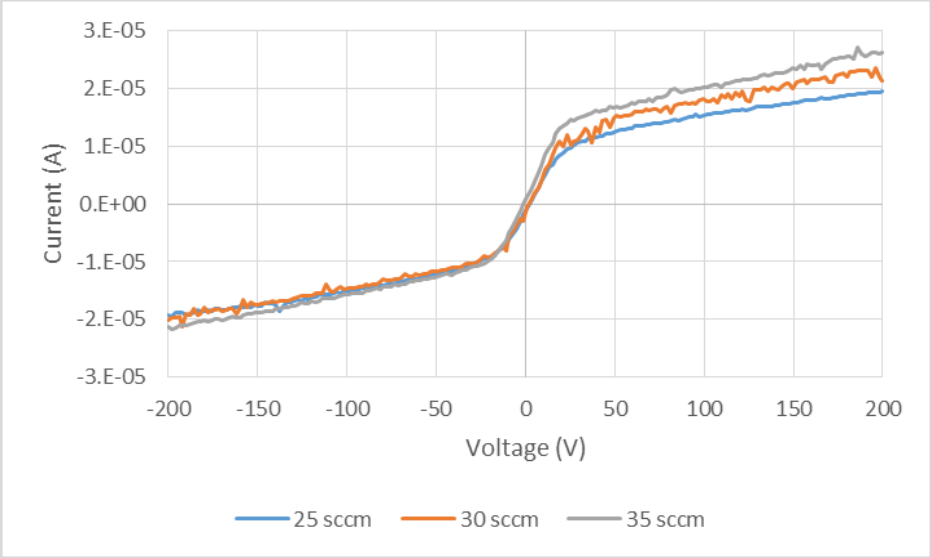

Figure 6. I-V curve for ac generated plasma at various flowrates.

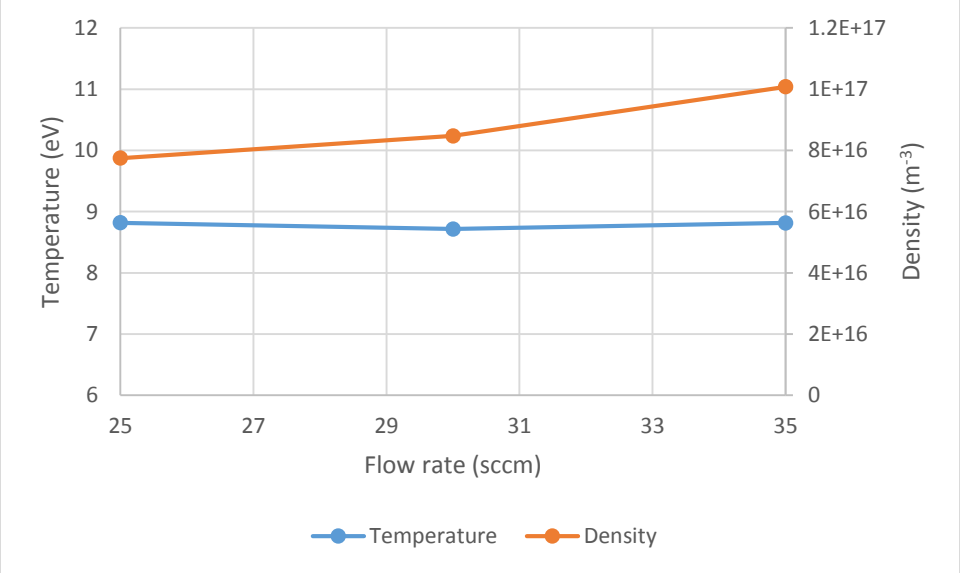

Figure 7. Ac generated plasma properties.

While the changes in flowrate did not affect electron temperature, an increased flowrate led to an increase in electron densities. Because the gas is the source of electrons, more flow allows for more ionization and therefore denser electrons.

The ac source cannot be varied, so flowrate is the only variable. The pulsed dc source provides more opportunities for optimization. Tests with the pulsed dc system allowed for variation in pulse width, frequency, and voltage in addition to variation in flow rate. After varying each of these, it was found that the most stable testing condition was a pulse width of 400 ns, frequency of 7 kHz, and voltage of 1.4 kV. The results from these tests can be seen in Figure 8.

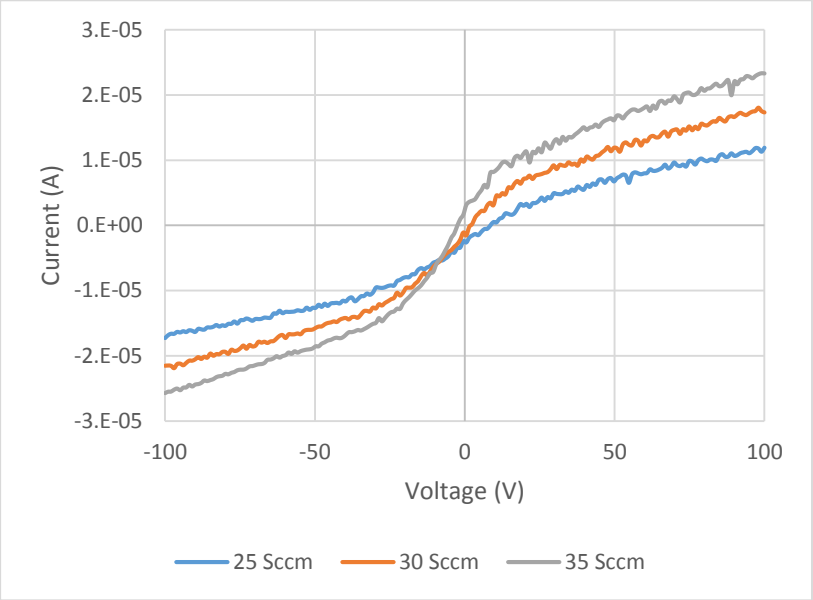

Figure 8. I-V curve for pulsed dc generated plasma at various flowrates.

As with the ac supply, the magnitude of the current steadily increases with flowrate. Equations 2 and 4 were used again to calculate the electron temperature and density for the unshielded cathode with an ion collector. The trends in electron temperature and density are shown in Figure 9.

While these conditions produced the steadiest plume, other conditions were also studied. The effects of varying voltage, pulse width, and frequency were explored. To study each of these, the flow rate was held constant at 30 sccm and each was varied individually. First, the voltage was set to 1.1 kV and 1.4 kV while the pulse width and frequency remained at 400 ns and 7 kHz, respectively. This resulted in the changes shown in Figure 10.

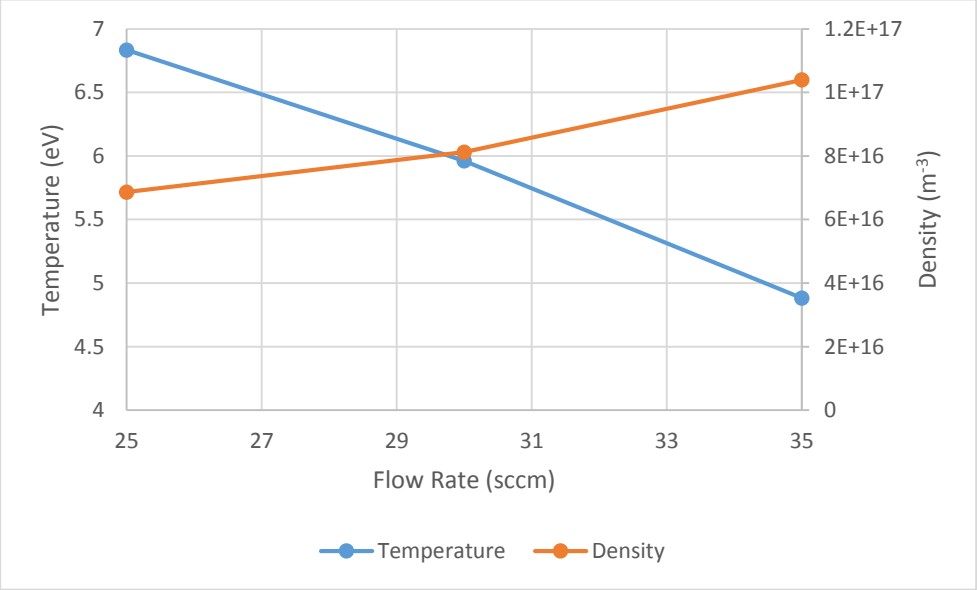

Figure 9. Pulses dc generated plasma properties.

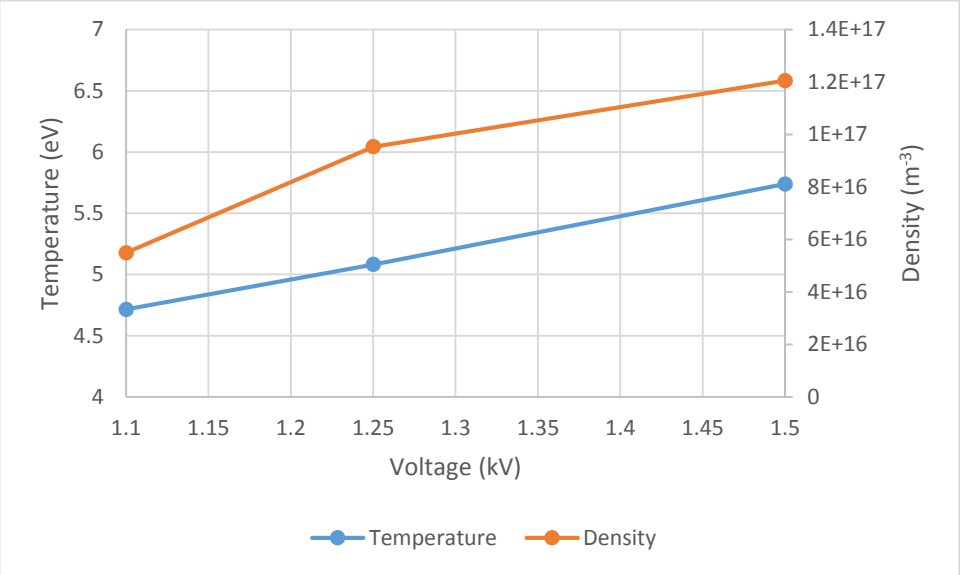

Figure 10. Variations in the input voltage to the cathode

Increasing the voltage to the cathode increased the electron temperature and density. With more power in the system, more ionization occurs. Increased ionization usually results in higher densities and lower temperatures, but increased power leads to higher temperatures as well. For the next test, the pulse width was set to 300 and 500 ns while the voltage remained at 1.25 kV and the frequency at 7 kHz. This resulted in the plot shown in Figure 11.

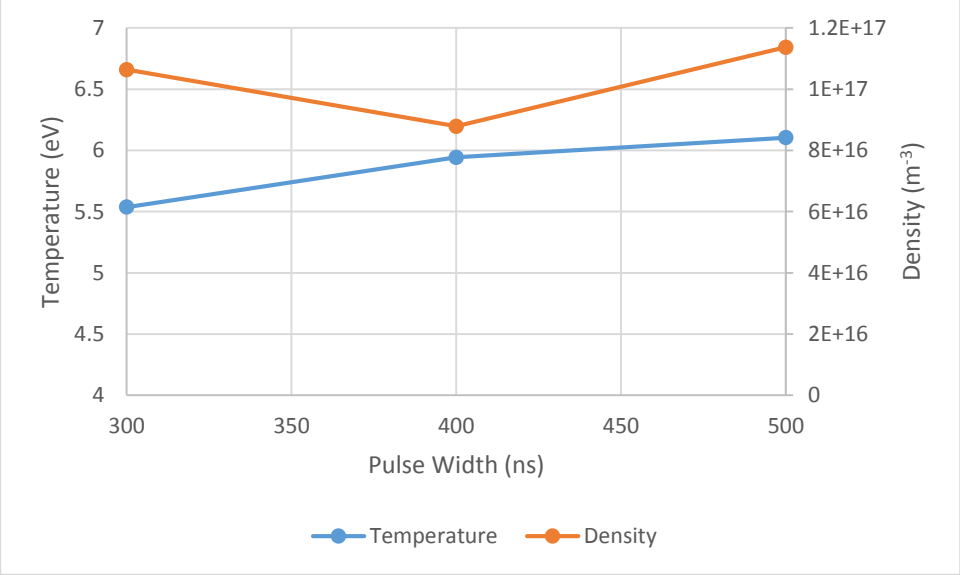

Figure 11. Variations in pulse width

Interestingly, while pulse width increases led to increases in temperature, pulse width did not largely affect density. This could be because the longer pulse times add more energy to the system, leading to higher temperatures. However,

the frequency of the pulses remained constant, meaning roughly the same amount of ionization occurred in these times. This led to little variation in density.

Finally, the pulse width was held at 400 ns and the voltage at 1.25 kV while the frequency was varied to 6 kHz and 8 kHz. These results are shown in Figure 12.

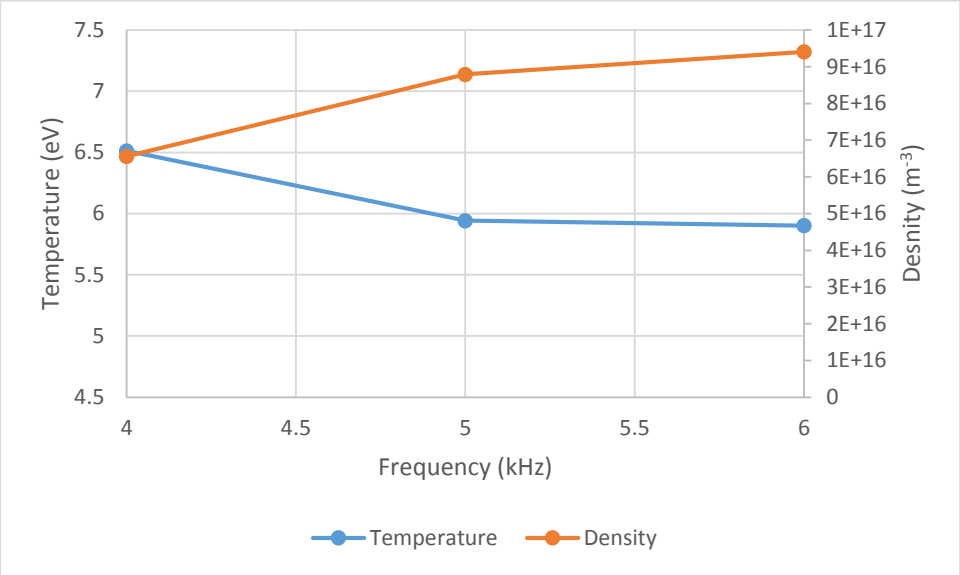

Figure 12. Variations in frequency

Frequency followed the trend of flow rate. As frequency increased, temperature decreased from 6.5 to 5.9 eV and density increased from 6.5 to 9.4e16 m^{-3}. As the pulses become more frequent, more ionization occurs in a shorter time. The plume also becomes visually brighter, as shown in Figure 13.

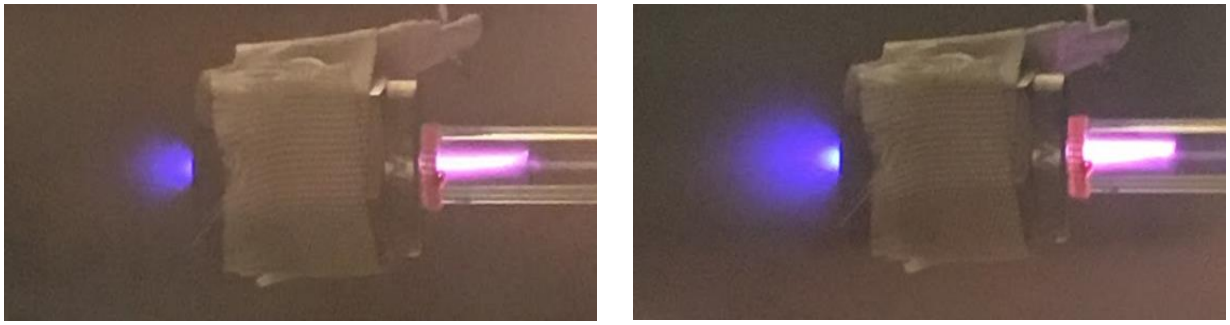

Figure 13. Changes from a weaker (left) to a stronger (right) plume.

Early testing of this cathode with a miniature Hall Thruster produced limited success. The setup and operation of this experiment can be seen in Figure 14. While a strong plume was drawn from the cathode into the thruster channel, currents above 10 mA could not be sustained. It is believed that currents of 100 mA or more are needed to sustain thruster ignition and operation. The densities of 10^{17} m^{-3} were not high enough to produce high currents. It is believed that this cathode could be more useful with the addition of a low work function insert material.

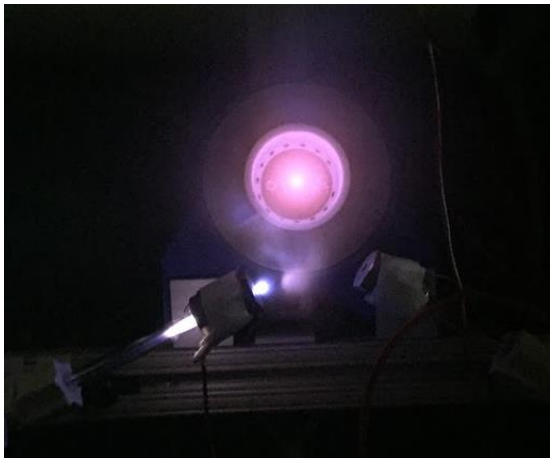

Figure 14. Hall thruster testing with heaterless, insertless cathode.

IV. Discussion

The heaterless, insertless cathode operated at a variety of conditions but was unable to produce high electron densities. It was generally found that at higher flow rates, frequencies, and voltages, higher densities were produced. However, even with the maximized condition, the highest density was found to be 1.5e17 m^{-3}. By assuming that the electron density in the plume is roughly equal to that inside the quartz tube, an estimation can be made of the maximum current flux in the quartz tube[7]. This calculation is shown in Equation 5.

$$\boldsymbol{\Gamma = A_T q n_e \left(\frac{8kT_e}{\pi M}\right)^{\frac{1}{2}}} \tag{5}$$

For an electron density of 1.5e17 m^{-3}, temperature of 4.2 eV, and tube diameter of 4 mm, the flux was calculated to be 1.6 mA. While the measured currents are around 10 mA, this approximate limit shows that a significant increase in density is needed to improve current output to the 100's of mA levels suitable for small thrusters. The difficultly with increasing the density, however, is that the operation range of the cathode with pulsed dc is limited by stability. It was found that limited ranges of operating conditions could produce a stable plume, and an even further limited range could produce a consistently steady plume. At higher voltages, for example, the plume would oscillate between a dim, weak plume, and a bright, strong plume. If the voltage got too high, the plume would transition into arc mode and cause damage to cathode elements.

This cathode design relies on the propellant gas as the source for the electrons. Therefore, the current is limited by the gas itself. Adding another electron source, such as an emissive material, could increase the electron density and therefore the current. Future tests will be conducted using thermionic materials such as molybdenum or tungsten wire as an insert material. Normal operation of this cathode produces high temperatures in the ion collector, and it is theorized that placing the molybdenum wire in the collector could cause the wire to reach its emission temperature.

V. Conclusion

Cathode operation has been verified in vacuum facilities at the University of Alabama in Huntsville. Variations were made in tube ID and OD, flow rate, power source, voltage, pulse width, and frequency. Measurements of the cathode plume with Langmuir probes determined the plasma properties. It was generally observed that higher flowrates, voltages, and frequencies led to higher electron densities. However, increasing flowrate and frequency lower the electron temperature. Measurements will be verified using Optical Emission Spectroscopy measurements in future tests.

References

[1] Longmier, B. W., and Hershkowitz, N., "Electrodeless Plasma Cathode for Neutralization of Ion Thrusters," *41st AIAA/ASME/SAE/ASEE Joint Propulsion Coference & Exhibit*, 2005, p. AIAA 2005-3856.

[2] Schatz, M. F., "Heaterless Ignition of Inert Gas Ion Thruster Hollow Cathodes," *AIAA/DGLR/JSASS 18th International Electric Propulsion Conference*, 1985, p. AIAA-85-2008.

[3] Aston, G., "Hollow cathode startup using a microplasma discharge," *Review of Scientific Instruments*, vol. 52, Aug. 1981, pp. 1259–1260.

[4] Vekselman, V., Krasik, Y., Gleizer, S., Gurovich, V., Warshavsky, A., Rabinovich, L., and Technion, "Characterization of a Heaterless Hollow Cathode," *Journal of Propulsion and Power*, vol. 29, 2013, pp. 475–486.

[5] Rubin, B., and Williams, J. D., "Hollow cathode conditioning and discharge initiation," *Journal of Applied Physics*, vol. 104, 2008.

[6] Chen, F., *Plasma Diagnostic Techniques*, New York: Academic Press Inc., 1965.

[7] Goebel, D. M., and Katz, I., *Fundamentals of Electric Propulsion: Ion and Hall Thrusters*, John Wiley and Sons, 2008.